SEISMIC ISOLATION RETROFIT OF LARGE HISTORIC BUILDING

By Anoop S. Mokha,[1] Navinchandra Amin,[2] Michael C. Constantinou,[3] and Victor Zayas,[4] Members, ASCE

ABSTRACT: Seismic isolation in the United States is gaining wide acceptance as an attractive and alternate means to upgrade historic structures seismically with minimal disturbance to architecturally significant features. One important historic-landmark structure that underwent such an upgrade is the Ninth Circuit U.S. Court of Appeals building located in San Francisco, which suffered damage during the 1989 Loma Prieta earthquake and was declared an unsafe building for further occupancy. The present paper summarizes the comprehensive approach adopted for implementation of the seismic-isolation technique for the seismic retrofit of this monumental structure. This historically significant structure is the first federal building to be retrofitted using seismic isolation. The paper discusses in detail the procedure adopted for evaluating the existing building strength, establishing the design approach, and evaluating and selecting the optimum isolator placement location and isolation system best suited for the building's structural performance and architectural usage.

Downloaded from ascelibrary.org by Rice University on 11/21/22. Copyright ASCE. For personal use only; all rights reserved.

INTRODUCTION

Few historic buildings meet current code seismic requirements for life safety, and most have architecturally significant elements that are threatened by future earthquakes. The first historic structure seismically retrofitted with base isolation, the Salt Lake City and County Building, drew attention to the use of isolation for sensitive existing buildings. Seismic isolation is now being proposed for more than a dozen historic structures in the United States.

Seismic isolation is a design technique that reduces the demand on structures by isolating them from the damaging effects of severe ground motions. The isolation is achieved with specially designed bearings that provide flexibility and energy absorption capability while supporting the weight of the structure. These bearings, which are replaceable if such need arises, are placed between the building and its foundation. Unlike conventional retrofitting schemes which rely on inelastic action of various structural elements to dissipate earthquake energy, the seismic isolation alternative reduces the force demand on the structure and thereby limits inelastic deformation. It provides a level of performance well beyond the normal code requirements with potential for substantial life-cycle cost reduction.

At present more than 300 structures worldwide have been constructed or are under construction on some form of isolation system. Seismic isolation systems are primarily classified into two basic types, one typified by elastomeric bearings and the other typified by sliding bearings. These systems have found application in most of the currently isolated structures. Other forms of isolation systems also exist, such as systems combining elastomeric and sliding systems, elastomeric bearings and fluid dampers, etc. (Kelly 1990; Anderson 1990; Skinner et al. 1993; Soong and Constantinou 1994). Elastomeric isolation systems function primarily by lengthening the period of the structure, thereby reducing the demand on the structure. The bearing displacements are controlled by use of either damping-enhanced rubber or by the use of additional energy dissipating elements such as mild steel dampers, lead plugs in the bearings, frictional elements, or viscous damping devices. Sliding systems function by limiting the transfer of force across the isolation interface. The restoring force is either integrated into the sliding unit or is provided externally (Soong and Constantinou 1994; Zayas et al. 1987; Mokha et al. 1991a).

The historic Ninth Circuit U.S. Court of Appeals at 7th and Mission Streets in San Francisco is owned by the General Services Administration (GSA). The building is a monumental structure of historical and architectural significance. The building suffered damage during the Loma Prieta earthquake of 1989 and was closed thereafter. It was recently retrofitted with seismic isolation and limited superstructure strengthening to provide a level of life safety and damage control beyond that of conventional strengthening methods. The friction pendulum isolation system was selected for the project. The present paper discusses the evaluation of several practical isolation systems and potential isolator locations for the Court of Appeals building. The design philosophy adopted for the project, the nonlinear dynamic analysis, isolation design, full-scale experimental verification of isolation system properties, and construction details are presented and discussed. Various implementation issues of interest to practicing engineers, such as long-term stability of the isolation-system properties and behavior of the isolated structure during minor and major earthquakes, are also discussed.

BUILDING DESCRIPTION

The original U-shaped building, constructed in 1905, structurally survived the devastating 1906 San Francisco earthquake and fire with minimal damage. In 1933, a fourth wing was added, giving the building a rectangular shape with a central atrium. Fig. 1 is a photograph of the building. Approximate plan dimensions are 100 m × 81 m (330 ft × 265 ft) and the total floor area is about 32,500 m^2 (350,000 sq ft). The building is a five-story, 24.4 m (80 ft) tall structure with steel framing, concrete slabs, unreinforced granite-masonry exterior walls and hollow clay tile interior partitions. The total weight of the building (dead load + reduced live load) is about 534 MN (120,000 kips). The interior finishes are extremely ornate and include carved marble figures, inlaid marble walls and floors, and highly articulated plaster ceilings (Fig. 2). This Beaux Arts building is on the National Register of Historic Places. At the completion of seismic retrofit in 1995, the Court of Appeals was the largest and the heaviest-base isolated building in the United States.

[1]Proj. Engr., Skidmore, Owings & Merrill, 333 Bush St., San Francisco, CA 94104.

[2]Chief Struct. Engr., Assoc. Partner, Skidmore, Owings & Merrill, 333 Bush St., San Francisco, CA.

[3]Prof., Dept. of Civ. Engrg., State Univ. of New York, Buffalo, NY 14260.

[4]Pres., Earthquake Protection Sys., Inc., 1045 Sansome St., Ste. 203, San Francisco, CA 94111.

Note. Associate Editor: Nicholas P. Jones. Discussion open until August 1, 1996. To extend the closing date one month, a written request must be filed with the ASCE Manager of Journals. The manuscript for this paper was submitted for review and possible publication on February 4, 1994. This paper is part of the ***Journal of Structural Engineering***, Vol. 122, No. 3, March, 1996. ©ASCE, ISSN 0733-9445/96/0003-0298–0308/$4.00 + $.50 per page. Paper No. 7761.

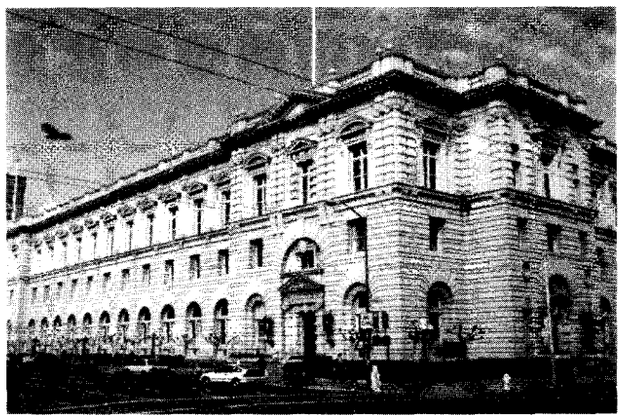

FIG. 1. U.S. Court of Appeals, San Francisco

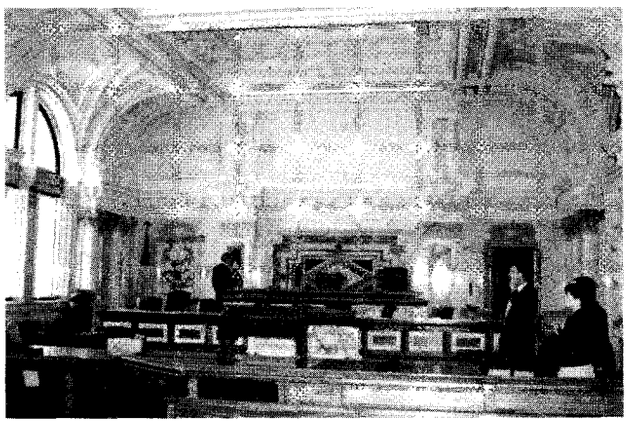

FIG. 2. Interior Finishes, U.S. Court of Appeals

The structural system for the 1905 U-shaped building consists of built-up columns with laced steel channels. The floor framing system consists of a beam-and-girder system, with beams spaced about 1.5 m (5 ft). Concrete slabs of arch-form span between the beams. Interior partitions walls consist of hollow clay tiles, and exterior walls are made up of unreinforced granite masonry supported by steel beams. The foundation consists of steel grillage footings encased in unreinforced concrete.

The structural system of the 1933 addition is entirely different from that of the 1905 building. The columns are made up of wide flange sections. The floor framing system consists of a beam-and-girder assemblage with 153 mm (6 in.) thick reinforced-concrete slab. Interior partitions are of hollow clay tiles and the exterior wall is made up of unreinforced-granite masonry. The foundation system for the 1933 wing consists of reinforced-concrete piles with reinforced-concrete pile caps.

EVALUATION OF EXISTING BUILDING

In any retrofit project the foremost problem the structural engineer is faced with is the evaluation of the existing structural strength and deformation capacity. Given the complexity of construction techniques and the use of various materials during the early part of this century, the answer cannot be reached by simple modeling of the structural system. This complexity leads to the next important issue: how close are we in assessing the dynamic characteristics of the existing structure? For nonhistoric structures, these issues are not very important since the primary intent of retrofit there is to provide life safety. For historically significant structures, where the performance objective extends beyond those of life safety and includes protection of architectural features, a reliable estimate of the existing structural capacity and of the dynamic characteristics of the structure is important.

TABLE 1. Summary of Various Tests and Application of Test Results to Establish Capacity of Existing Structure

	Results Based on Tested Material or System			
Type of test (1)	Brick masonry (2)	Granite masonry (3)	Hollow clay tile partition wall (4)	Existing structure (5)
Compressive strength	5.86–13.44 MPa[a]	82.74–91.70 MPa[b]	—	—
Shear strength	0.67–0.70 MPa[a]	1.16–2.15 MPa[b]	—	—
Out-of-plane strength	—	0.6 g[c]	0.5 g[c]	—
Forced vibration	—	—	—	$T_s = 0.57$ s[d] $\xi = 2.5\%–5\%$ of critical[d]

[a]Applied to lateral capacity of brick wall at basement level.
[b]Applied to lateral capacity of structure above basement level and to overturning capacity of granite piers.
[c]Applied to out-of-plane acceleration limit and deflection limit.
[d]For confirmation of analytical model of structure for small-amplitude vibration.

TABLE 2. Measured Frequencies of Building and Comparison to Values Predicted Analytically

Mode Number (1)	Measured frequency (Hz) (2)	Observed mode shape (3)	Calculated frequency (Hz) (4)
1	1.76	First E-W	2.17
2	1.92	First N-S	2.69
3	2.16	First torsional	3.24

An extensive testing program was undertaken to determine the strength of the various components of the existing building. The tests used cores of concrete slabs, exterior stone and brick masonry to determine their compressive and shear strength, and steel coupons to determine the yield strength of steel. In-place shear tests were performed on brick and stone masonry to evaluate the existing lateral-force–resisting capacity of the building. Out-of-plane stone masonry panels were tested by applying pressure with air bags to determine the out-of-plane capacity of the walls. An in-place shear racking test was done on an exterior stone masonry panel and an interior hollow clay tile partition wall. A summary of various tests, their results, and application of test results is presented in Table 1.

To evaluate the dynamic characteristics of the existing building, forced vibration tests were carried out. The existing structure was excited by a 20.5 kN (4,600 lb) eccentric mass shaker and the structural response was recorded through accelerometers at various locations. From the recorded response, the frequencies, mode shapes, and damping values were obtained under conditions of small-amplitude vibration. Table 2 presents the measured frequencies of the first three modes of the building. The corresponding damping ratios were estimated to be 2.5% to 5% of critical. Moreover, tests were performed in order to evaluate the interaction between the old 1905 building and the 1933 addition. No measurable differential motion was recorded for excitations with frequency below 5 Hz.

The dynamic properties of the structure were determined in low-amplitude tests, which involved peak accelerations on the order of 0.001 g. This level of excitation, which is barely into the range of human perceptibility, is significantly less than the expected response of the isolated structure, in which accelerations are on the order of 0.35 g. Extrapolation of the low-level data to the seismic response level required the review of

J. Struct. Eng., 1996, 122(3): 298-308

Downloaded from ascelibrary.org by Rice University on 11/21/22. Copyright ASCE. For personal use only; all rights reserved.

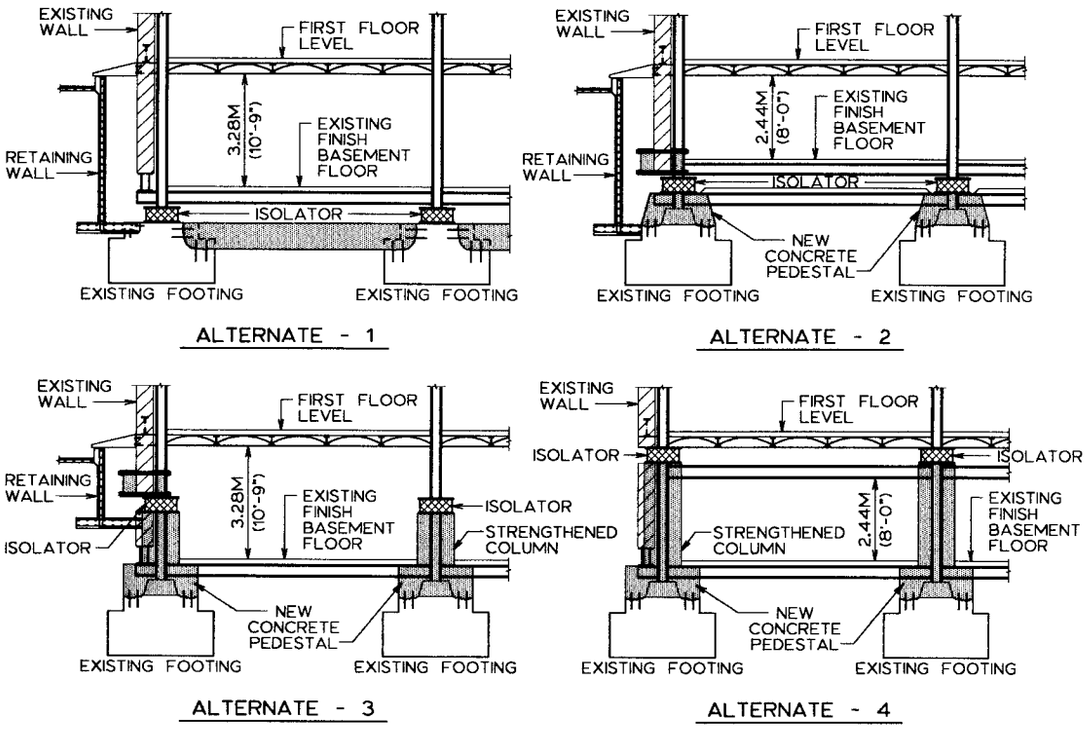

FIG. 3. Various Options for Locating Isolator Plane

past earthquake response, evaluation of load paths, and engineering judgment.

Analyses of the structure indicated that its stiffness was dominated by the stiffness of the outer granite walls, which act as shear walls. Observations from the 1906 and 1989 earthquakes indicated that the granite walls and mortar suffered significant damage. It was concluded that the measured dynamical properties of the structure prior to its retrofit would not significantly change in a high-level earthquake as long as the granite walls and mortar do not fail in a significant number of locations. Rather, the expected behavior would be mild softening with the fundamental period increasing by about 25% and the damping ratio by about 50% to 100%. Thus, expected values of fundamental period and damping ratio of the structure prior to its retrofit and for a high-level earthquake would be about 0.70 s and 5% to 10% of critical, respectively (Keowen et al. 1995).

The retrofit scheme of the U.S. Court of Appeals included, in addition to seismic isolation, strengthening of the superstructure. That is, shear walls were added to carry about 50% of the calculated structural shear force under elastic conditions, diaphragms were strengthened, and a new moment resisting frame was built for the atrium. The shear walls were strategically placed to minimize the effect on the architectural features of the structures. Overall, the superstructure was strengthened to the point that it could sustain elastically or near elastically the calculated seismic forces and drifts. The dynamical properties of the strengthened superstructure were expected to be close to those obtained in the forced vibration testing. However, the measured properties were not directly used in modeling the superstructure. Rather, they were used in confirming the various assumptions made in the analytical modeling of the superstructure.

EVALUATION OF ISOLATION SYSTEMS AND LOCATIONS

Two related issues must be addressed early in the isolation design process. The first concerns the location of the plane of isolation, and the second concerns the isolation system to be used. For historic buildings, proper consideration of these issues should lead to minimization of retrofit cost and to meeting the functionality and architectural preservation goals of the structure.

For the Court of Appeals building, an extensive series of studies were performed to evaluate the effect of different isolation systems and isolator locations. The effects of the various considered isolation systems on the response of the isolated superstructure, on the nonstructural design requirements, and on the interdisciplinary coordination were considered in these parametric studies.

Four locations for the isolation plane were studied (Fig. 3):

1. Alternate 1—above the foundation and below the basement
2. Alternate 2—just above the basement slab
3. Alternate 3—at mid-height of the basement columns
4. Alternate 4—at the top of the basement columns

The goal of these studies was to evaluate the costs associated with the performance and installation of isolators at these four alternate locations.

Isolator Location

A complex matrix of costs and impacts was developed to evaluate each alternate isolator location. For each of the four locations, excavation costs, moat requirements, architectural and mechanical impact, overall constructability, and the amount of superstructure strengthening that would be required were determined.

Alternate 1 (above the foundation and below the basement slab) was selected as the optimum isolator location because it provided sufficient headroom in the basement for the architectural program, efficient installation, and minimal disruption to mechanical, electrical, and plumbing services. Alternates 2, 3, and 4 were less desirable architecturally and more disruptive to building services. Most importantly, they would have required more strengthening and involved details, which would require higher costs and a longer construction schedule. To

Downloaded from ascelibrary.org by Rice University on 11/21/22. Copyright ASCE. For personal use only; all rights reserved.

complete alternate 1, additional tie beams connect the footings below the plane of isolation, and a new basement floor slab serves as a rigid diaphragm just above the isolators.

Isolation System

The owner (General Services Administration) solicited competitive technical bid proposals to select and procure the isolation system for the Court of Appeals project (Palfalvi et al. 1993). The document contained separate specifications and pricing tables for three types of isolation systems: high damping rubber bearing, lead rubber bearing and the friction pendulum system (FPS). These isolation systems were determined to be acceptable products by an earlier study. The solicitation required offerers to submit unit prices for the various quantities for the particular bearings proposed. Preliminary testing specifications were also provided. In the bid documents, bearing sizes and quantity were provided for all three isolation systems. As the design progressed, the original isolation system designs were refined. The reanalysis and redesigning of the candidate isolation systems was necessary in order to evaluate the impact of acceptable types of isolator on the superstructure response, architecture, and other disciplines. The main intent of these studies was to facilitate the complex issues of accommodating the acceptable types of isolators and comparing their performance to common parameters. For example, the height of the isolators had an important impact on cost and construction time since tall bearings required lowering of the existing pile caps in order to maintain minimum headroom requirements in the 1933 wing of the building.

Technical considerations and pricing were finally the dominant factors in the selection of the friction pendulum system for this project.

Nonlinear Dynamic Analysis

Nonlinear dynamic time-history analyses were performed to evaluate the performance of the isolation system and superstructure for each of the three isolation system designs. Fig. 4 shows the mathematical model of the isolated structure. The model was developed in computer code 3D-BASIS (Nagarajaiah et al. 1991). It consisted of three degrees of freedom per floor and an explicit multidirectional nonlinear element for each isolation bearing.

Three pairs of ground-motion time histories were provided by the project geotechnical consultant and used as input motion for the nonlinear analysis. The peak ground acceleration of these motions was $0.4g$. These time histories were developed from the following recorded ground motions after scaling to match the site-specific spectrum (developed to have a 10% probability of being exceeded in 50 years):

1. Loma Prieta Earthquake—Santa Cruz Record (TH-1 and 2)
2. Michoacan Earthquake—La Union Record (TH-3 and 4)
3. Loma Prieta Earthquake—Capitola Record (TH-5 and 6)

For each ground motion, the two time histories were applied simultaneously to simulate bidirectional movement. For example, TH-1 was applied in the x-direction while TH-2 was applied in the y-direction. Each pair was also switched, i.e., TH-2 was applied in the x-direction and TH-1 in the y-direction. The effect of bidirectional movement on the response of the isolation system and isolated structure is significant enough to be considered in the analysis and design of an isolated structure (Mokha et al. 1993).

The elastic properties of the superstructure were condensed from a detailed three-dimensional model developed in computer code SAP90 (Wilson et al. 1989). In this detailed model, floors were modeled as flexible diaphragms. The fundamental period of the nonisolated structural model was calculated to be 0.46 s. This period is less than the period of 0.57 s obtained in the forced vibration test. Degradation of the existing structural stiffness during the Loma Prieta earthquake explains the longer period obtained in the forced vibration tests. Table 2 shows a comparison of the free vibrational characteristics of the structure as obtained by forced vibration testing on the existing structure and by analysis of the retrofitted structure. The higher frequencies calculated for the first three fundamental modes are attributed to the stiffness contribution of new shear walls. The superstructure was assumed to remain elastic with a damping ratio of 5% of critical in each mode of vibration.

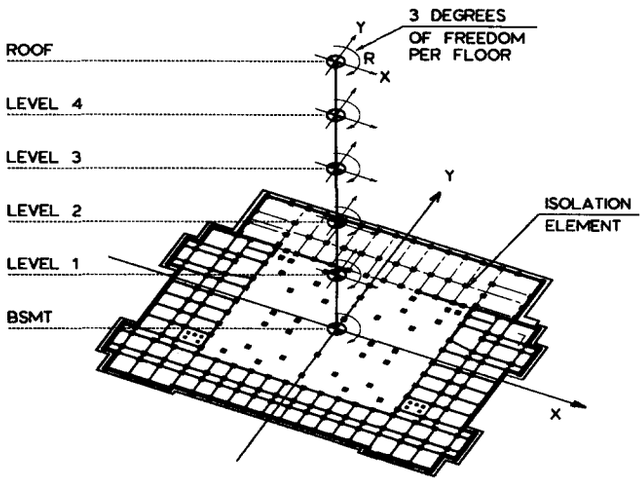

FIG. 4. Model for Dynamic Analysis of Isolated Structure

IMPLEMENTATION OF FPS BEARINGS

Description of FPS Bearings

The FPS bearing consists of an articulated slider on a concave spherical stainless-steel surface. A cross-sectional view of the FPS isolator of the U.S. Court of Appeals building and connection details is shown in Fig. 5. Dimensions are given in Table 3. Characteristics of these bearings are the polished stainless-steel spherical sliding surface and the articulated slider that is faced with a PTFE-based, high bearing-capacity composite material. The bearings are typically sealed and installed with the sliding surface facing down, so that contamination of the sliding interface is avoided.

The FPS bearing acts as a fuse, activated only when the shear force across the isolation interface overcomes the static friction force. Once in motion, the articulated slider moves along the concave spherical surface, causing the supported mass to rise, with motions equivalent to those of a simple pendulum. The kinematics and operation of the bearing is the same whether the concave is facing up or down. Geometry and gravity achieve the desired seismic-isolation results. During the rise along the spherical surface the bearing develops a lateral resisting force equal to the combination of the mobilized frictional force and a gravity-induced restoring force. That is, the lateral force is equal to

$$F = (W/R)u + \mu W \operatorname{sgn}(\dot{u}) \tag{1}$$

where u = bearing displacement; $\dot{u}$ = bearing sliding velocity; W = supported weight; R = radius of curvature of spherical surface; and μ = coefficient of sliding friction. Thus, the lateral force is directly proportional to the supported weight. This causes the center of stiffness and lateral resistance of the bear-

Downloaded from ascelibrary.org by Rice University on 11/21/22. Copyright ASCE. For personal use only; all rights reserved.

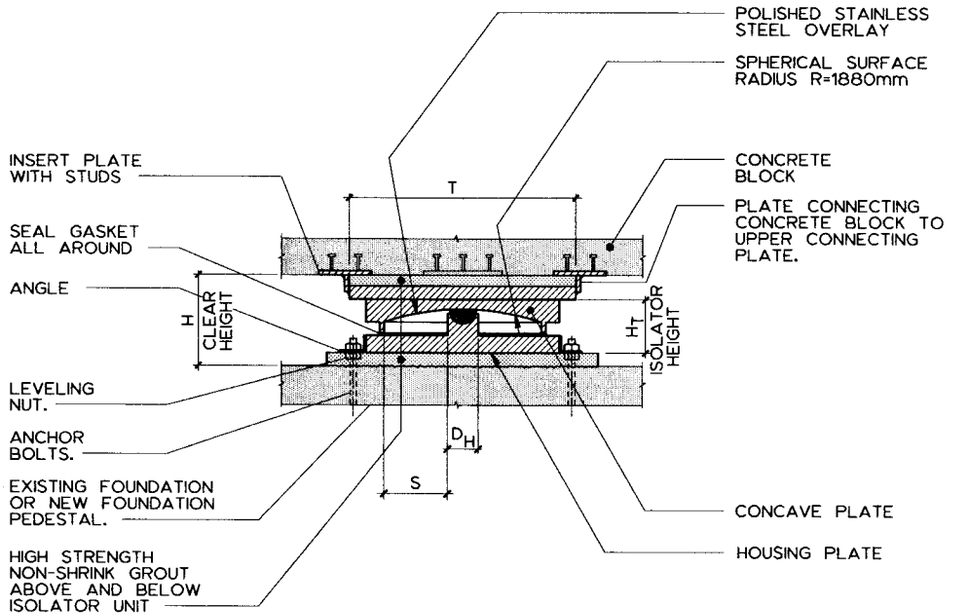

FIG. 5. Cross-Sectional View of FPS Bearings of the U.S. Court of Appeals Building

TABLE 3. Dimensions, Displacement Capacities, and Range of Loads of FPS Bearings for U.S. Court of Appeals

Bearing type (1)	Number (2)	Dimensions (mm) T^b (3)	H_T^c (4)	H^d (5)	D_H^e (6)	Displacement Capacity S (mm) (7)	Range of Load (kN)[a] (8)
A	26	1,070	250	430	125	350	445–890
B	10	1,070	250	430	125	350	890–1,335
C	52	1,120	250	445	175	350	1,335–1,780
D	42	1,120	250	445	175	350	1,780–2,225
E	62	1,170	250	460	225	350	2,225–2,670
F	41	1,170	250	460	225	350	2,670–3,115
G	22	1,220	290	500	275	350	3,115–4,450
G1	1	1,220	290	500	275	350	5,340

[a]Dead and live load only.
[b]Plan dimension.
[c]Height of isolator.
[d]Total height.
[e]Diameter of contact area.

ing group to coincide directly with the center of mass of the supported structure, thus compensating for mass eccentricities. This property minimizes torsional motion of the supported structure, which often causes severe damage to structures.

Once the threshold of static friction is exceeded, the structure responds at its isolated period, with the dynamic response and damping controlled by the isolator properties. The natural period of vibration of an FPS-isolated structure is independent of the building weight and is given by

$$T_b = 2\pi(R/g)^{1/2} \tag{2}$$

where g = acceleration of gravity.

The coefficient of sliding friction in FPS bearings follows the relation (Constantinou et al. 1990)

$$\mu = f_{max} - (f_{max} - f_{min})\exp(-a|\dot{u}|) \tag{3}$$

where f_{max} = value of coefficient of friction at high velocity of sliding; f_{min} = value at very low sliding velocity; and a = parameter that controls the variation of the coefficient of friction with the velocity of sliding. Typically, f_{max} is dependent on the bearing pressure and its attained at velocities exceeding about 50 mm/s (that is, parameter a equals to about 0.1 to 0.2 s/mm).

Fig. 6 presents values of coefficients friction f_{min}, f_{max} and μ_B (breakaway or static value) of FPS bearings as measured in four different test programs (Zayas et al. 1987; Al-Hussaini et al. 1994; Constantinou et al. 1993), and in the tests of the prototype bearings of the U.S. Court of Appeals. Typically in the FPS bearings the static friction is less than the value at high velocity of sliding, f_{max}. The controlling value f_{max} has values between about 0.12 and 0.05, depending on the bearing pressure. It should be noted that the test results in Fig. 6 extend over a range of bearing pressure of about 17 MPa to 275 MPa (2.5 to 40 ksi). The polytetrafluoroethylene (PTFE) composite used in the FPS bearings, which was originally developed for military and aerospace applications, is rated to pressures of about 300 MPa and has an ultimate capacity of over 415 MPa (60 ksi).

Vertical ground accelerations and overturning moments cause fluctuations in the axial load carried by the bearings. The effect of varying axial load is twofold. First, the mechanical properties of the bearing are affected (e.g., an instantaneous increase in axial load results in an instantaneous increase in stiffness and friction force). Second, the design forces for the bearings and foundation are affected. Under extreme conditions uplift may occur, which needs to be evaluated.

At the time of analysis and design of the isolation system

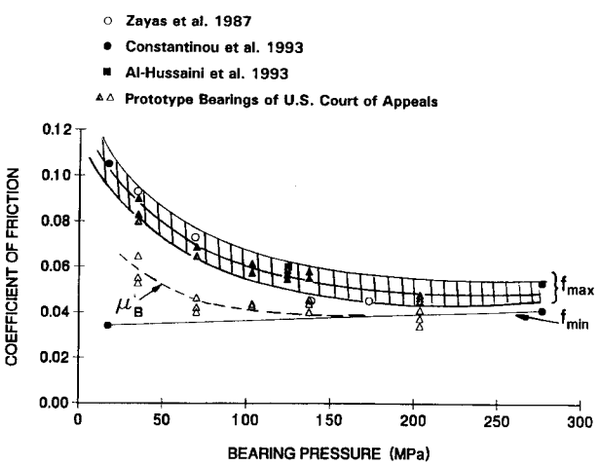

FIG. 6. Frictional Properties of FPS Bearings

Downloaded from ascelibrary.org by Rice University on 11/21/22. Copyright ASCE. For personal use only; all rights reserved.

of the U.S. Court of Appeals building, the instantaneous effects of varying axial force could not be explicitly modeled. This capability became available only recently (Tsopelas et al. 1994). The approach followed was to account implicitly for these effects in the following way. Since the relation between vertical load and horizontal force of the bearings is substantially linear, the net effect of overturning moment on the mechanical behavior of a group of bearings was assumed to be small and it was neglected. Shake table testing of an isolated seven-story building model subsequently confirmed this hypothesis under extreme conditions of vertical load, which included bearing uplift (Al-Hussaini et al. 1994).

The effect of vertical ground acceleration (peak value of $0.27g$) is to change the gravity load on each bearing from the static value W to a minimum value of 0.73 W and a maximum value of 1.27 W. However, these values are not indicative of the effect on the bearing behavior unless the vertical and horizontal earthquake components are perfectly correlated. To reflect more realistically this random correlation, it was assumed that the axial load on each bearing had a value of either W or 0.90 W or 1.10 W (based on the 100% + 40% combination rule). The most important effect of this variation is on the value of the friction force, which was accounted for by analyses with a coefficient of friction equal to the design value and values of 1.1 or 0.9 times the design value.

The effects of overturning moment and vertical ground acceleration on bearing forces were determined in the following way. Dynamic analyses of the isolated structure resulted in histories of acceleration of the degrees of freedom shown in Fig. 4. At selected instances of time (i.e., times of maximum bearing displacement, maximum floor acceleration, maximum structural shear force, and maximum overturning moment), these accelerations were converted to inertia forces and applied as static loads to a detailed model of the structure, in which the isolation bearings were modeled as pins. The analysis resulted in maximum and minimum axial loads on the bearings, which were subsequently increased or decreased by a 10% amount to account for vertical acceleration effects. The analysis showed that the minimum load on all bearing was compressive (no uplift occurred). The maximum axial load was substituted in (1) to obtain, for the design displacement, a conservative estimate of the lateral bearing force. This pair of maximum axial and lateral forces was used in the design of the bearings and foundations.

A study was recently conducted to evaluate by a rigorous method the potential for uplift of the bearings of the U.S. Court of Appeals building (Wang et al. 1995). The study confirmed that uplift does not occur in the design level earthquake. The same study also determined that uplift of less than 1 mm could occur in the bearings supporting the most slender shear walls (height-to-length ratio of 5) in the maximum capable earthquake. This uplift displacement is too small to cause dislodgement of the bearings (see Al-Hussaini et al. 1994 for experimental data).

Isolation System Configuration

The final design called for the use of 256 FPS bearings of eight types. Dimensions and range of loads for each type of bearing are included in Fig. 5 and Table 3. The total number of each bearing type is also shown in Table 3. A radius of curvature of 1,880 mm (74 in.) was selected to achieve the design isolation period of 2.75 s. The design coefficient of friction f_{max} was selected as 0.07 for sliding velocities greater than 50 mm/s (2 in./sec).

Design Approach

The nonisolated structure was initially analyzed with records of the 1989 Loma Prieta earthquake extrapolated to the site. The records were developed by the geotechnical engineer considering site characteristics and recorded motions at nearby sites. The results of these dynamic analyses were correlated to the observed damage in the Loma Prieta earthquake. This damage consisted of cracking of the exterior granite cladding, dislodgment and/or cracking of marble wainscots, severe cracking of hollow clay tile walls, and weakening of the lateral load resisting system. Based on these results, the performance criteria of the isolated structure were established. Table 4 lists the calculated peak response of the nonisolated structure in the Loma Prieta earthquake, the observed damage and the established performance criteria of the isolated structure for the design-level earthquake (a 475-year event, i.e., an earthquake that has a 10% probability of being exceeded in 50 years).

TABLE 4. Peak Response of Nonisolated Structure in Loma Prieta Earthquake, and Performance Criteria of Isolated Structure

Parameters (1)	Calculated response (2)	Performance criteria for isolated structure (3)
Structure shear force (% of weight)	20.30	≤16.00
Peak interstory drift ratio (% of column height)	0.53	≤0.20
Maximum floor acceleration (g)	0.48	≤0.40

Following the establishment of the desired performance criteria, the isolated structure was analyzed for the Loma Prieta input, as extrapolated to the site and scaled by factors 1.0, 1.5, and 2.0, and the design-level earthquake scaled up by a factor of 1.2 to represent the maximum capable earthquake. The results are presented in Table 5, where they are compared against the response of the nonisolated structure. The significant benefits offered by seismic isolation are evident in the results of Table 5. The isolated structure has a calculated response approximately five times lower than that of the nonisolated structure in the design-level earthquake. Moreover, this response of the isolated structure in the design earthquake is less than that of the nonisolated structure in the much weaker Loma Prieta earthquake.

The calculated response of the isolated structure in the Loma Prieta earthquake is also substantially less (by a factor of 2.5) than that of the nonisolated structure. Furthermore, the response of the isolated structure in the maximum capable earthquake approaches that of the nonisolated structure in the Loma Prieta earthquake. Since the lateral load resisting system of the structure is strengthened in the seismic isolation retrofit, it is expected that the isolated structure will not suffer any damage in the design level earthquake and suffer only some nonstructural damage in the maximum capable earthquake.

The FPS bearings have been designed to have a maximum displacement capacity of 350 mm (Table 3), which exceeds the calculated demand for the maximum level earthquake (345 mm). Thus, the outside rims enclosing the concave steel surface of the FPS bearings (Fig. 5) do not serve as displacement restrainers. Rather they are useful in sealing the sliding interface.

Consideration of Long Term Properties of FPS Bearings

A concern regarding the application of seismic isolation is the long-term reliability of the properties of the isolation bearings. Given that inevitably the properties of all materials and devices change with time, a study was conducted to assess possible variations in the properties of FPS bearings, to establish manufacturing and installation procedures that could en-

Downloaded from ascelibrary.org by Rice University on 11/21/22. Copyright ASCE. For personal use only; all rights reserved.

TABLE 5. Calculated Response of Fixed and Isolated U.S. Court of Appeals Building

Event (1)	Low level earthquake (2)				Design level earthquake (3)		Maximum capable earthquake (4)
Earthquake	LP	LP	1.5 LP	2 LP	DL	DL	1.2 DL
Peak ground acceleration (g)	0.10	0.10	0.15	0.20	0.40	0.40	0.48
Structure	Fixed	Isolated	Isolated	Isolated	Fixed	Isolated	Isolated
Maximum structure shear (% of weight)	20.30	7.78	9.46	11.11	81.30	15.60	20.30
Maximum floor acceleration (g)	0.48	0.19	0.23	0.23	2.27	0.35	0.47
Maximum interstory drift ratio (% of column height)	0.53	0.07	0.08	0.08	0.80	0.11	0.12
Maximum bearing displacement (mm)	—	41.9	88.9	139.7	—	268.5	344.9

Note: LP = Loma Prieta Earthquake and DL = Design-Level Earthquake.

Downloaded from ascelibrary.org by Rice University on 11/21/22. Copyright ASCE. For personal use only; all rights reserved.

hance longevity and to assess the impact of hypothetical changes of properties on the response of the isolated structure.

The conclusions of the conducted study were as follows:

1. The actual stiffness of FPS bearings is entirely controlled by the geometry of the bearings, and thus unchangeable with time.
2. The only potential change could occur in the coefficient of friction as a result of the following: contamination of the sliding interface, corrosion of stainless steel, deterioration of the PTFE-based composite material, and dwell of load.
3. Contamination is preventable because FPS bearings are completely sealed. However, it was decided to install the bearings with the spherical surface facing down, so that collection on the surface of debris from within the sealed space would be avoided. Possible contamination of the sliding surface during installation was mitigated by specifying that the bearings be assembled and sealed in a dust-free environment and not disassembled during installation. Moreover, the bearing seals were preloaded so that they could remain closed for vertical bearing displacement of up to 2 mm. For the FPS bearings with radius of curvature of 1,880 mm, a bearing vertical displacement of 2 mm is reached when the horizontal displacement is 87 mm. However, the bearing construction (Fig. 5) is such that the seal opens at a horizontal displacement of 75 mm (seal moves at the edge of the housing plate). Thus, the bearings are expected to remain sealed in low magnitude earthquakes. When displacements exceed the limit 75 mm (the structure is instrumented with mechanical displacement recorders) inspections are required to verify that the seals are intact.
4. Based on limited available data, deterioration of the PTFE-based composite material of the sliding interface was not considered to be problematic. Particularly, the material was known to have unique inertness and chemically stability.
5. Data on corrosion of stainless steel were collected from a variety of sources and an inventory of polished stainless parts was examined. The inventory included seven parts in storage for 34 years under conditions equivalent to sealed FPS bearings. All parts were in excellent condition with perfectly reflective finish. The interested reader is referred to Soong and Constantinou (1994) for a more detailed description. Based on the collected data, a decision was made to use the stainless steel with the best observed performance, that is, highly polished austenitic type-316L stainless steel (American 1987). Furthermore, the conditions of assembly of the FPS bearings were specified so that lifetime could be prolonged (e.g., avoidance of welding of stainless steel and cleaning of stainless steel from all iron particles with acid).
6. Dwell of load (that is, loading of the bearing without any movement for prolonged time) was thought to have an effect on the static value of friction. Mokha et al. (1991b) conducted tests on unfilled PTFE and woven PTFE and studied the effect of dwell of load for times up to 594 d. The tests demonstrated that the static friction coefficient remained unchanged. Based on these and other results, Soong and Constantinou (1994) provided a physically motivated description of the phenomenon. According to this theory, dwell of load affects the friction force primarily through an increase of the true contact area due to viscoelastic effects. The effect occurs within a short time interval (minutes to a few hours) depending on the type of materials and bearing pressure. At sufficiently high pressure (above approximately 10 MPa) the true contact area equals the geometric bearing area and dwell of load has insignificant effects on the mobilized friction force. The bearings of the U.S. Court of Appeals building were designed at a bearing pressure of at least 70 MPa.

Based on the conducted study it was concluded that variations in the frictional properties of the FPS bearings were likely to be only minor. To assess their effect, minor variations of coefficient of friction f_{max} in the range of 0.06 to 0.08 (e.g., $\pm 15\%$ of the design value) were considered. The results of analyses are presented in Table 6. The calculated response exhibits minor changes and remains within the specified performance criteria of Table 4. Furthermore, for the purpose of

TABLE 6. Effect of Variation of Coefficient of Friction on Peak Response in Design-Level Earthquake

Parameters (1)	Minor changes in friction coefficient: Case 1 (2)	Case 2 (3)	Case 3 (4)	Major changes in friction: Case 4 (5)	Case 5 (6)
Maximum Coefficient of Friction, f_{max} (%)	6	7	8	10.50	14
Minimum Coefficient of Friction, f_{min} (%)	3.50	4.50	5.0	6.75	9
Maximum Structure Shear (% of weight)	16.10	15.60	14.80	14.50	15.67
Maximum Floor Acceleration (g)	0.30	0.35	0.39	0.39	0.49
Maximum Interstory Drift Ratio (% of column height)	0.11	0.11	0.10	0.13	0.17
Maximum Bearing Displacement (mm)	298.7	268.5	237.7	143.5	96.5

demonstrating to the owner the reliability of the system, analyses were performed for hypothetical increases of the friction coefficient by 50% and 100% of the design value. The results are presented in Table 6. For 100% increase in the friction coefficient, the response in terms of structure shear force and interstory drift are still within the specified performance criteria. The peak floor acceleration reaches the level calculated for the nonisolated structure in the Loma Prieta earthquake. It was thus demonstrated that an unanticipated major change of the coefficient of friction will most probably not result in damage to the structural system. Finally, a comprehensive testing program has been developed in which three bearings will be loaded and stored at the site and tested after 2, 5, and 12 years.

Installation of FPS Bearings

The architectural and historical significance of the existing building imposed difficult requirements for installing isolation bearings under the existing columns. Given the configuration of existing columns as pairs of channels laced together and carrying an average axial load of 2,700 to 4,000 kN (600 to 900 kips), lifting of columns required a special arrangement. Fig. 7 shows a typical interior column with an FPS bearing installed. The existing columns were encased in reinforced concrete and a reinforced-concrete block, typically 2 m wide and 2.4 m long, was constructed close to the isolator location. The concrete encasement served two purposes: it increased the capacity of existing columns to sustain seismic P-delta effects safely and provided permanent lifting blocks for future jacking (for bearing removal for testing or replacement). As previously discussed, the installation of FPS bearings with the concave surface facing down was a design decision arrived at by consideration of long-term maintenance and performance of FPS bearings. Furthermore, in this installation method, the point of application of the axial bearing load does not move with bearing lateral movement, thereby reducing the strengthening demand on the foundations of the existing building.

The installation of FPS bearings were achieved as follows. After the concrete encasement was cast and cured, four symmetrically placed hydraulic jacks with jacking stools were positioned under the concrete block. The pairs of jacks were placed 1.83 m apart. Dial gauges were provided under the column, at the ends of concrete blocks and on the column above. Based on the estimated gravity load in the column, hydraulic pressure was applied gradually to the jacks. With the dial gauges being monitored, the lifting operation was continued until the dial gauge under the column showed the column being lifted. At this stage, the four jacks were locked using the collar nut and the hydraulic pressure was released. The jacking stools were designed to have an ultimate load of three times the estimated gravity load. The existing column was then cut at approximately 20 mm from the bottom of the concrete block using torch flame. The cut piece of column was then removed and the isolator was inserted in the space between the concrete block and the foundation. The isolator was then levelled to a tolerance of about 0.15° and grouted at the top and bottom. A tight tolerance of 0.75 mm on the vertical upward movement of the existing column during the lifting operation was specified to protect the historic fabric of the building. Also a limit on the jacking load of 110% of the estimated load in the column was specified, so that existing columns were not overstressed. Throughout the lifting operation the jacking load never exceeded 90% of the estimated load.

The simplicity of the lifting operation resulted in rapid installation of the FPS bearings at an average rate of eight bearings per week by a single group of four workers. The 256 bearings were installed in less than six months.

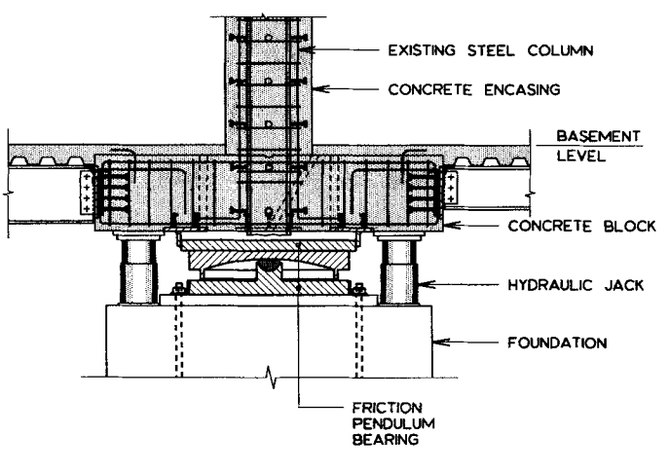

FIG. 7. Installation Details of FPS Bearing under Interior Columns

FULL-SCALE EXPERIMENTAL VERIFICATION OF FPS BEARING PROPERTIES

For the successful implementation of any isolation system, experimental verification of design properties is necessary. Unlike conventional structural materials like steel and concrete for which engineering properties are well documented in codes and manuals, the properties of isolation systems are not yet documented. This lack of information dictates the need for evaluation of isolation system properties for any given project. For the Court of Appeals building an extensive testing program was developed to test full-size FPS bearings for validation of assumed design parameters.

Testing Requirements

Three sets of testing specifications were developed for materials, prototype, and production bearings. The material test specifications were intended to quantify the frictional properties of the bearings. Prototype-bearings testing requirements were extensive and primarily intended to test full-size bearings under dynamic conditions expected during an earthquake. The production-bearing testing specifications were designed to confirm that each bearing delivered the desired properties. The main characteristics of the material, prototype, and production bearings testing were as follows:

1. All bearings were tested at full design loads.
2. Bearings were tested at velocities of 50.8, 127, 254, and 508 mm/s (2, 5, 10, and 20 in./sec).
3. Bearings were tested at 0.25, 0.5, 0.75, and 1.0 times the design displacement of 268.5 mm (10.57 in.).
4. All tests consisted of three cycles of loading.
5. Endurance tests were performed with ten cycles of loading at 1.2 times the design displacement.
6. Bearings were also tested with variable axial load.
7. All 21 prototype bearings and 256 production bearings were tested.

Despite a rigorous quality-control program established for the manufacture and assembly of the bearings, all 256 production bearings were tested to ensure that each and every bearing satisfied the project specifications. The requirement for dynamic testing at high velocities up to 508 mm/s was specified with a two-fold intent:

- To observe the behavior of the bearings under conditions for which they have been designed
- To evaluate the integrity of the entire bearing assembly under severe dynamic loading

Downloaded from ascelibrary.org by Rice University on 11/21/22. Copyright ASCE. For personal use only; all rights reserved.

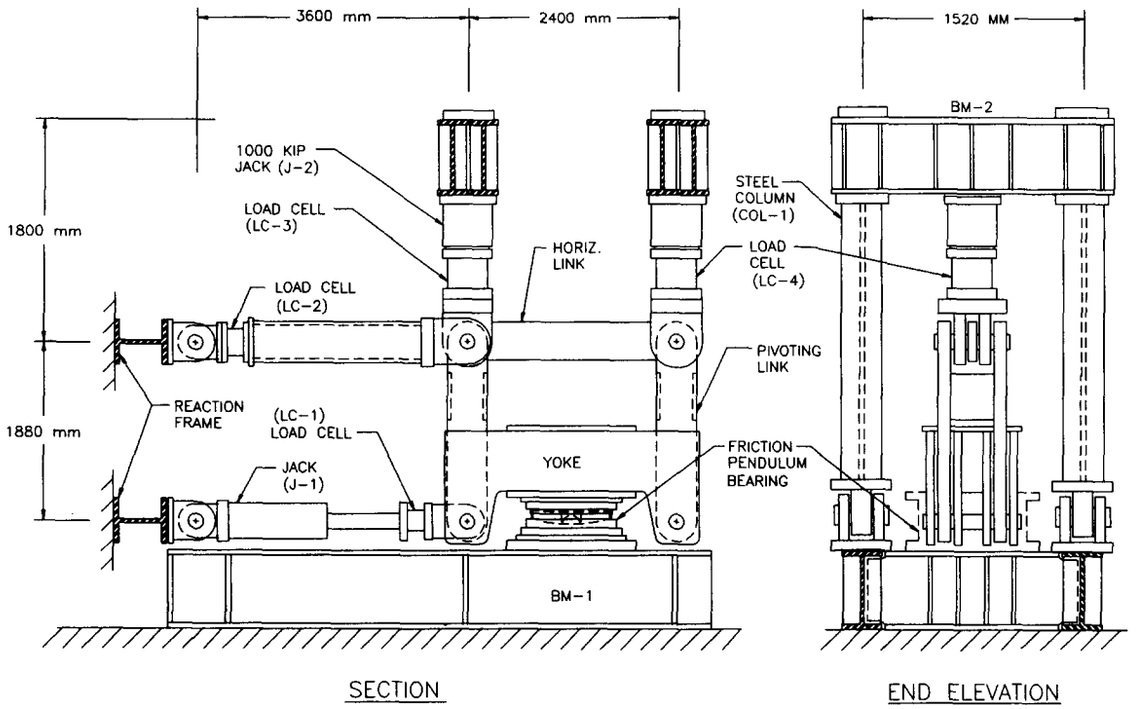

FIG. 8. Schematic of Test Machine

These dynamic testing requirements for full-size production bearings, which are not typically performed for isolation projects in the United States, provided the designers and owner with confidence and an understanding of the isolation system.

Testing Arrangement

A testing machine was designed to meet the loading requirements for the material, prototype, and production testing of full-size FPS isolators. A schematic representation of the test machine is shown in Fig. 8. The figure shows the basic moving elements, loading arrangement, and the outer frame designed to provide the necessary reactions to the hydraulic-jack loadings and for the overall stability of the machine.

The portion of an FPS bearing with a concave surface is bolted down to the rigid slab resting on heavy beams BM-1. The remaining portion containing the articulated slider is bolted to a yoke, which is suspended by pivoting steel links (truss action). The normal load at the interface of the slider and the concave surface is maintained by two vertical load jacks (J-2) with the reaction coming from four columns COL-1 via beams BM-2. A jack (J-1) through a horizontal ram applies displacement controlled horizontal load on the yoke. The yoke can swing horizontally. The adjustable length of the pivoting links is set equal to the radius of the concave surface of the FPS bearing (1880 mm for the bearings of the U.S. Court of Appeals). As a result, when the yoke moves horizontally, the restoring force developed in the FPS bearing is equal to the horizontal component of the axial force in the arms. The restoring force is resisted and measured by the upper horizontal load cells (LC-2). The friction force is measured by the lower horizontal load cell (LC-1). The vertical load is recorded through two load cells (LC-3 and LC-4). A displacement transducer records the movement of the horizontal ram. Two accelerometers were also attached to the yoke to measure accelerations.

This testing machine designed for the U.S. Court of Appeals project is capable of delivering up to 8,900 kN (2,000 kips) of axial load and about 2,225 kN (500 kips) of shear load. Stroke is ±381 mm (15 in.) at velocities of up to 508 mm/s

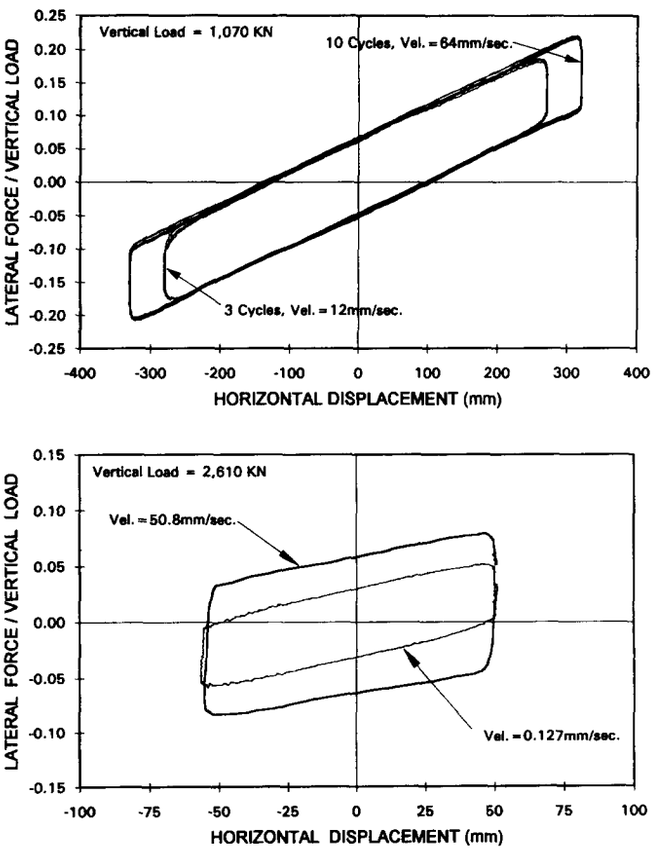

FIG. 9. Force Displacement Hysteresis Loops of Full-Size FPS Bearings

(20 in./sec.). Fig. 9 shows 3 and 10 cycles of force-displacement hysteresis loops of a type B FPS isolator (see Table 3) at vertical load of 1,070 kN (240 kips), amplitude of 270 mm and 330 mm, and peak velocities of 12 mm/s and 64 mm/s, respectively. Bearing pressure is 86 MPa. Both force-displace-

Downloaded from ascelibrary.org by Rice University on 11/21/22. Copyright ASCE. For personal use only; all rights reserved.

ment hysteresis loops show consistent and repeatable behavior without any degradation of frictional and stiffness properties. Through such force-displacement hysteresis loops for all 256 production bearings, it was demonstrated that the bearings as designed satisfied the project's performance criteria. Fig. 9 also shows one cycle of force-displacement hysteresis loop for a type E FPS isolator at vertical load of 2,610 kN (585 kips), amplitude of 55 mm, and peak velocities of 0.127 mm/s and 50.8 mm/s. The velocity dependence of the coefficient of sliding friction should be noted.

Shake Table Test with Full-Size FPS Bearings

The design of the isolation system, the utilized analytical model, and the predicted seismic performance, were verified with earthquake simulation tests of unreinforced masonry structural models. The tests were conducted on the shake table at the Earthquake Engineering Research Center of the University of California, Berkeley. The test structure consisted of a full-scale one-story steel frame with unreinforced masonry infill panels. The test structure was supported on full-size FPS isolation bearings. The masonry-panel specimens consisted of unreinforced granite, double-width brick, and single-width brick panels. The isolated structure with the masonry panels was subjected to over 200 shake table tests. Earthquake simulation included the design ground motions for the U.S. Court of Appeals and simulations of strong (magnitude 8) earthquakes, which exceeded the design-level earthquake. None of the masonry infill specimens showed any cracking or damage after these severe and repeated seismic loadings. After completing the isolated model tests, the isolation bearings were locked up by attaching the side plates used for shipping. The fixed base (nonisolated) models with the masonry panels were then subjected to earthquake loadings. All of the masonry panels suffered severe damage during these fixed base tests, even though the strength of the applied earthquake loadings was less than that applied to the isolated models. A more detailed description of these tests may be found in Zayas et al. (1993).

CONCLUSIONS

The implementation of seismic isolation for retrofitting of an historic structure has been presented. Based on the various parametric studies performed for various isolation systems and the design approach used for the U.S. Court of Appeals, the following is concluded:

1. Seismic isolation retrofit can effectively achieve life-safety criteria and minimize damage to the ornate architectural features of historic buildings.
2. Systematic evaluation of isolator location and isolator type can result in considerable cost savings. Sacrificing building areas for the implementation of an isolation system creates a significant economic burden for the project. For the U.S. Court of Appeals building the systematic evaluation of the isolator location and type resulted not only in considerable cost savings but also the availability of the entire basement area for building and tenant use.
3. For existing historic structures, such studies identify early on in the project the problems associated with installation and performance of various isolation systems.
4. For historic buildings, the selection of the isolation system should be based on the existing constraints, desired superstructure performance, and the overall economics.
5. The analysis for any isolation system should include design assumptions that are verified through a full-scale test of prototype and production bearings.
6. The structural implications of long term variations of isolation system properties should be taken into account in the design.
7. It is important to test full-size isolators to anticipated realistic motions in order to verify the assumptions employed in the design.

ACKNOWLEDGMENTS

The writers wish to thank the General Services Administration for permitting publication of this work. Thanks are also owed to Hamid Fatehi, Peter Lee, Xiaoxuan Qi, Emilio Alejandria and Rich Nelson of Skidmore, Owings & Merrill for their contribution to the project. The contribution of Mason Walters of Forell/Elsesser Engineers, Bela Palfalvi of the General Services Administration, and Stanley Low of Earthquake Protection Systems is also appreciated. Two anonymous ASCE reviewers provided comments that greatly improved the paper. Their contribution is appreciated.

The design of the U.S. Court of Appeals building won the 1994 General Services Administration National Award for Engineering, Technology, and Innovation.

APPENDIX. REFERENCES

Al-Hussaini, T. M., Zayas, V. A., and Constantinou, M. C. (1994). "Seismic isolation of multi-story frame structures using spherical sliding isolation systems." *Report No. NCEER-94-0007*, Nat. Ctr. for Earthquake Engrg., Buffalo, N.Y.

American Society for Metals. (1987). *Metals Handbook, Corrosion. Vol. 13, 9th Ed.*, Metals Park, Ohio.

Anderson, T. L., ed. (1990). "Theme issue: seismic isolation." *Earthquake Spectra*, 6(2), Earthquake Engineering Research Institute, Oakland, Calif.

Constantinou, M. C., Mokha, A., and Reinhorn, A. M. (1990). "Teflon bearings in base isolation, part 2." *J. Struct. Engrg.*, ASCE, 116(2), 455–474.

Constantinou, M. C., Tsopelas, P., Kim, Y-S., and Okamoto, S. (1993). NCEER-Taisei Corporation research program on sliding seismic isolation systems for bridges: experimental and analytical study of friction pendulum system (FPS)." *Report No. NCEER-93-0020*, Nat. Ctr. for Earthquake Engrg., Buffalo, N.Y.

Kelly, J. M. (1990). "Base isolation: linear theory and design." *Earthquake Spectra*, 6(2), 223–244.

Keowen, S., Amin, N., Mokha, A., and Ibanez, P. (1995). "Vibration study of the U.S. Court of Appeals building for seismic isolation retrofit." *Proc., 1st World Conf. on Struct. Control*, Int. Assoc. for Struct. Control, Los Angeles, Calif., WP4-103–WP4-112.

Mokha, A., Constantinou, M. C., Reinhorn, A. M., and Zayas, V. (1991a). "Experimental study of friction pendulum isolation system." *J. Struct. Engrg.*, ASCE, 117(4), 1201–1217.

Mokha, A., Constantinou, M. C., and Reinhorn, A. M. (1991b). "Further results on the frictional properties of teflon bearings." *J. Struct. Engrg.*, ASCE, 117(2), 622–626.

Mokha, A., Constantinou, M. C., and Reinhorn, A. M. (1993). "Verification of friction model of Teflon bearings under triaxial load." *J. Struct. Engrg.*, ASCE, 119(1), 240–261.

Nagarajaiah, S., Reinhorn, A. M., and Constantinou, M. C. (1991). "3D-BASIS non-linear dynamic analysis of three dimensional base isolated structures: Part II." *Report No. NCEER-91-0005*, Nat. Ctr. for Earthquake Engrg. Res., Buffalo, N.Y.

Palfalvi, B., Amin, N., Mokha, A., Fatehi, H., and Lee, P. (1993). "Implementation issues in seismic isolation retrofit of government buildings." *Proc., Seminar on Seismic Isolation, Passive Energy Dissipation and Active Control, Vol. 1, ATC 17-1*, Appl. Technol. Council, Redwood, Calif., 257–264.

Skinner, R. I., Robinson, W. H., and McVerry, G. H. (1993). *An introduction to seismic isolation.* John Wiley and Sons, Inc., Chichester, England.

Soong, T. T., and Constantinou, M. C., eds. (1994). *Passive and active structural vibration control in civil engineering*, Springer-Verlag, New York, N.Y.

Tsopelas, P. C., Constantinou, M. C., and Reinhorn, A. M., (1994). "3D-BASIS-ME computer program for nonlinear dynamic analysis of seismically isolated single and multiple structures and liquid storage tanks." *Rep. No. NCEER-94-0010*, Nat. Ctr. for Earthquake Engrg. Res., Buffalo, N.Y.

Downloaded from ascelibrary.org by Rice University on 11/21/22. Copyright ASCE. For personal use only; all rights reserved.

Wang, X.-F., Amin, N., and Mokha, A. (1995). "Study of base uplift of seismic isolated building." *Symp. on Nat. Hazard Phenomena and Mitigation, ASME/JSME/PVP Conf.*, ASME, New York, N.Y., 155–160.
Wilson, E. L., and Habibullah, A. (1989). *SAP-90—a series of computer programs for the static and dynamic analysis of structures*. Computers and Structures, Inc., Berkeley, Calif.
Zayas, V., Low, S., and Mahin, S. (1987). "The FPS earthquake resisting system." *Rep. No. UCB/EERC-87/01*, Earthquake Engrg. Res. Ctr., Berkeley, Calif.
Zayas, V. A., Piepenbrock, T., and Al-Hussaini, T. (1993). "Summary of testing of the friction pendulum seismic isolation system 1986-1993." *Proc., Seminar on Seismic Isolation, Passive Energy Dissipation and Active Control, Vol. 1, ATC 17-1*, Appl. Technol. Council, Redwood, Calif., 377–388.

Downloaded from ascelibrary.org by Rice University on 11/21/22. Copyright ASCE. For personal use only; all rights reserved.